Hardware and methods of the optical end-to-end test of the Far Ultraviolet Spectroscopic Explorer (FUSE)

Steven J. Conard [*a], Kevin W. Redman[b], Robert H. Barkhouser[a], Doug B. McGuffey[c], Stephen Smee[d], Raymond G. Ohl[†a], Gary D. Kushner[e]

[a] Department of Physics and Astronomy, The Johns Hopkins University

[b] ManTech Systems Engineering Corporation, Goddard Space Flight Center, Greenbelt, MD

[c] Swales Aerospace, Inc., Beltsville, MD

[d] National Institute of Standards and Technology, Gaithersburg, MD

[e] Center for Astrophysics and Space Astronomy, University of Colorado

ABSTRACT

The Far Ultraviolet Spectroscopic Explorer (FUSE), successfully launched in June 1999, is an astrophysics satellite designed to provide high spectral resolving power ($\lambda/\Delta\lambda$ = 24,000--30,000) over the interval 90.5--118.7 nm. The FUSE optical path consists of four co-aligned, normal incidence, off-axis parabolic primary mirrors which illuminate separate Rowland circle spectrograph channels equipped with holographic gratings and delay line microchannel plate detectors.

We describe the hardware and methods used for the optical "end-to-end" test of the FUSE instrument during satellite integration and test. Cost and schedule constraints forced us to devise a simplified version of the planned optical test which occurred in parallel with satellite thermal-vacuum testing. The optical test employed a collimator assembly which consisted of four co-aligned, 381 mm diameter Cassegrain telescopes positioned above the FUSE instrument, providing a collimated beam for each optical channel. A windowed UV light source, remotely adjustable in three axes, was mounted at the focal plane of each collimator.

Problems with the UV light sources, including high f-number and window failures, were the only major difficulties encountered during the test. The test succeeded in uncovering a significant problem with the secondary structure used for the instrument cavity and, furthermore, showed that the mechanical solution was successful. The hardware was also used extensively for simulations of science observations, providing both UV light for spectra and visible light for the fine error sensor camera.

KEY WORDS: FUSE, optical testing, alignment, ultraviolet, calibration

1. INTRODUCTION

The Far Ultraviolet Spectroscopic Explorer (FUSE) is a NASA satellite program that will obtain high resolution ($\lambda/\Delta\lambda$=24,000--30,000), far-ultraviolet (FUV; 90.5--118.7 nm) spectra from astronomical sources. It was conceived and fabricated by The Johns Hopkins University (JHU) and an international team of corporations, universities, and government agencies.[1] It was launched in June 1999 aboard a Delta II rocket from the Cape Canaveral Air Force Station.

[*] Correspondence: Email: sjc@pha.jhu.edu; WWW: http:/fuse.pha.jhu.edu/; Telephone: 410-516-8390, Fax: 410-516-5494

[†] Also at Astronomy Department, University of Virginia

FUSE consists of four coaligned telescopes, which each direct FUV photons into the slits of separate Rowland circle spectrographs. The spectrographs were developed and aligned at the University of Colorado.[2] The telescopes were aligned to the spectrograph using non-FUV techniques, as described elsewhere.[3]

We discuss the hardware and procedure used to execute the optical "end-to-end" test (OETET) of the FUSE instrument. This test was complicated by a number of critical issues, including directing both visible and FUV photons into the system, remotely operating the test hardware in a vacuum chamber, and schedule and cost control. The OETET was executed late 1998 and early 1999 at NASA/Goddard Space Flight Center (GSFC).

The OETET was not intended to perform a complete radiometric and wavelength calibration of the FUSE instrument. Its more limited objectives were three-fold:

- show that the optical system had no gross defects
- provide stimuli to the system to support flight simulations
- provide an environment for testing in-flight optical alignment techniques

The transmission of FUV photons requires high vacuum conditions. The OETET therefore necessitated a large vacuum chamber. To help minimize cost and schedule impact, the test was combined with the satellite-level thermal-vacuum test.

2. TEST METHOD

2.1 Original concept

When the FUSE instrument was redesigned to its current configuration (changed from grazing incidence to normal incidence optics), the baseline was to design and fabricate a vacuum chamber and UV collimation system to permit both alignment and characterization. Later, FUSE was further cost-constrained, and it was decided to abandon this baseline in favor of a less costly method.

2.2 Final concept

Like almost all satellites, FUSE required a thermal-vacuum (TV) test at the system level. An existing large vacuum chamber at GSFC had already been identified for this purpose. We decided to combine the OETET with the TV test. Some immediate advantages were realized:

- The cost of constructing a separate vacuum chamber for each test (i.e. the TV test and OETET) was eliminated.
- The OETET would occur later in the integration and test process, allowing data obtained to be closer to "as launched."
- This plan would allow flight-like testing at the full satellite level of assembly.

2.3 Associated risk

We incurred a number of additional risks by combining the OETET and the TV test, including:

- While testing closer to launch, we risked finding a problem that would require disassembly of the satellite to repair.
- The configuration of the chamber required mounting the light sources completely within vacuum. Therefore, the lamps had to be self-contained, sealed units (the window material limited the lower wavelength cutoff to >105.0 nm) and they would not be accessible during the test, which proved to be a critical limitation.
- Light source motions would have to be remotely controlled via drive mechanisms qualified for the vacuum environment.
- The collimating optics and light sources would be suspended above the satellite.

3. COLLIMATOR ASSEMBLY DESIGN

The OETET optical path is shown schematically in Figure 1. An optical assembly consisting of four UV collimators, one per channel, is suspended above the FUSE instrument inside the Solar Environment Simulator (SES).[4] Each collimator produces a FUV output beam with ~λ/20 RMS wavefront error (λ = 632.8 nm) and many strong emission lines over the interval 105 < λ < 120 nm, sufficient to meet the science-driven requirements for the optical test (Figure 2). The collimator optical assembly is mechanically referenced to the top of FUSE via four post flexures and the majority of the assembly weight is off-loaded by a counterbalance, which is integral to the supporting superstructure (Figure 3).

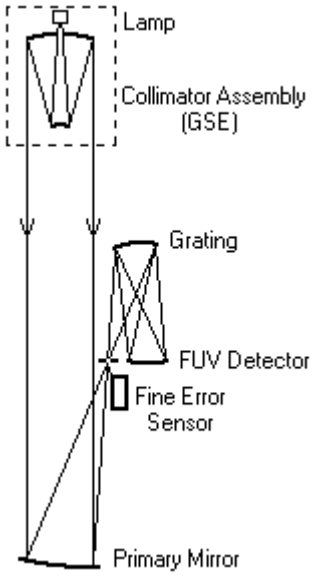

Figure 1 Optical Path

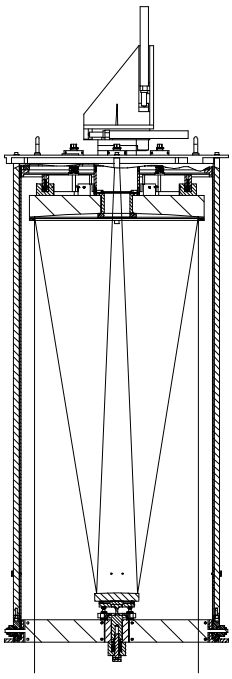

Figure 2 Collimator Assembly

The rationale for this "suspended" test configuration stems from the need to perform the OETET in conjunction with thermal vacuum testing. In this environment, the optical system is particularly susceptible to misalignment caused by transient thermal gradients within the supporting structure; an inevitable consequence of the temperature cycling that occurs during thermal testing. Rather than having a support structure that provides both load support as well as a mechanical reference to the satellite, these roles have been separated. Here, the low CTE carbon-fiber-composite structure of the FUSE instrument is used as the mechanical reference maintaining optical alignment, while the majority of the optical assembly load is carried by a cable attached to a counterweight mechanism. In this fashion, optical alignment is maintained with little susceptibility to satellite motion or changes in the thermal environment and the deleterious effects of mass loading on the instrument are abated by the support structure. In addition, the need to erect scaffolding and mount cryo-panels around the periphery of the satellite greatly limited the feasibility of a thermally stable (invar or composite) floor-mounted support structure.

3.1 Collimators

Each collimator is a f/12 classical Cassegrain design with a 381 mm diameter clear aperture (Figure 2). The Zerodur primary is supported via a nine-point whiffle tree mount with tip-tilt adjustment. The secondary is mounted on a tip/tilt/translation stage centered on a traditional four-bladed spider support. Invar metering rods establish the primary--secondary spacing. To reduce cost, the collimator tubes were fabricated from aluminum. Heaters were placed on the bottom of the tube as well as the spider blades to balance the heat loss from the collimator aperture. A pinhole at the base of a Pt-Ne hollow-cathode lamp mounted on a three-axis stage provides a "steerable" light source at the focal plane.

3.2 Optical bench

The optical bench supports the individual collimators and establishes the interface with the FUSE instrument (Figure 3). Kinematic "V-groove" mounts, three per collimator, are used to coalign the four individual channels. Post flexures on precision translators at the base of the optical bench facilitate attachment and alignment with the instrument. Thin aluminum panels with film heaters and multi-layer insulation enclose the aluminum plate structure and the collimators to maintain a 20°C operating temperature. Approximately 90% of the optical bench/collimator weight is off-loaded from the FUSE instrument via a single cable which extends from the counterbalance of the overhead superstructure (Figure 4). Load cells at the base of each post flexure monitor load transmitted to the instrument.

3.3 Superstructure

The superstructure provides the primary load support for the collimator structure (Figure 3). The basic arrangement emulates a bridge crane and is supported by

outriggers attached to the chamber wall. The interface between the superstructure and the outriggers is kinematic to allow for thermal expansion during testing; no heaters are placed on this part of the system. A balance beam arrangement was used to suspend the collimator assembly and negate the effects of changes in cable length, satellite motions, chamber motions, etc. An adjustable counterweight bucket was attached at one end of the beam and the collimator assembly was hung over a pulley at the other end. This balance beam assembly was situated on the trolley bridge frame, which allowed adjustment of the position of the collimator assembly relative to the satellite.

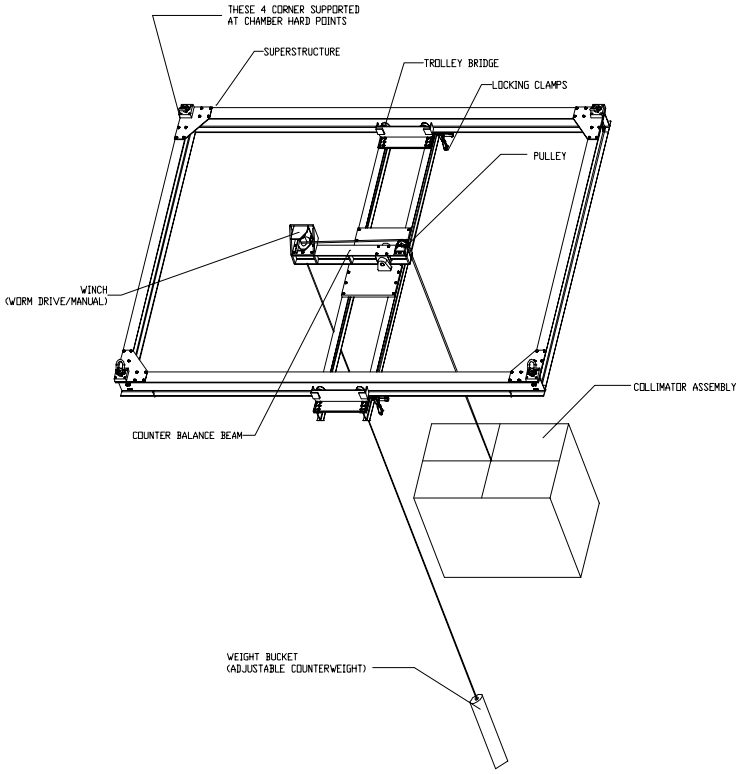

Figure 3 Support Superstructure

4. COLLIMATOR ALIGNMENT AND COALIGNMENT

4.1. Collimator alignment

The collimators were designed to be used in a vertical configuration, with optical axes parallel to the gravity vector. No provision was available to hold them horizontally for alignment and then rotate to vertical for the OETET, so we assembled and aligned all four units in their OETET configuration. With slight modifications, our method for aligning each collimator is described elsewhere.[5]

Initially the cell holding the primary mirror was installed in the end of the aluminum collimator tube along with the tube adjustment mounts (Figure 5). The tube adjustment mount allowed the rotation of the collimator in pitch and yaw. The tube and mirror were then lifted and placed in a telescope support table, which held the collimator vertically and provided a stable, kinematic mount for the duration of the assembly and alignment process. The tube adjustment mounts interfaced to tooling balls in V-blocks attached to the support mount. The axis of the tube was coarsely leveled to gravity by placing a bubble level on the primary mirror cell backplate and adjusting the mounts until centered. At this point, theodolites were used to record the elevation readings of two adjacent faces of an optical cube bonded on the primary mirror cell backplate. This cube and elevation readings would later be used to co-align the collimators to each other.

The next step was to align the primary mirror's optical axis to gravity reference. A line-of sight through the collimator tube was needed which would define the gravity vector and the center of the primary mirror aperture. A circular target with centered crosshairs was installed in the primary mirror cell central aperture to mechanically define the optical axis, relying on design tolerances. A mercury pool level was then placed under the tube on the telescope support mount. The mercury pool provides a “mirror surface” whose normal always points straight up. A 45° relay mirror was then installed on the primary mirror cell backplate such that it folded the mercury pool normal horizontally in a convenient direction. A theodolite was then positioned where it could autocollimate on the mercury pool via the relay mirror while centered on the circular plug crosshairs. This process put the theodolite in position to define the nominal location and pointing direction of the collimator optical axis. From here the theodolite was maintained in position and undisturbed while the mercury pool level was removed. This allowed the theodolite to look through the telescope support mount to another 45° mirror based on the floor which again turned the theodolite line-of-sight horizontally (Figure 6). The lower relay mirror was large enough (400 mm diameter) to cover approximately 70% of the collimator aperture. This was important, because it allowed us to place a fiber optic point source on a translator assembly near the folded center of curvature of the primary mirror. Thus positioned, the point source illuminated the primary mirror, which reflected the light back through the lower relay mirror, returning to a point at or near the fiber source. At this point, the goal was to adjust the fiber source in focus such that the

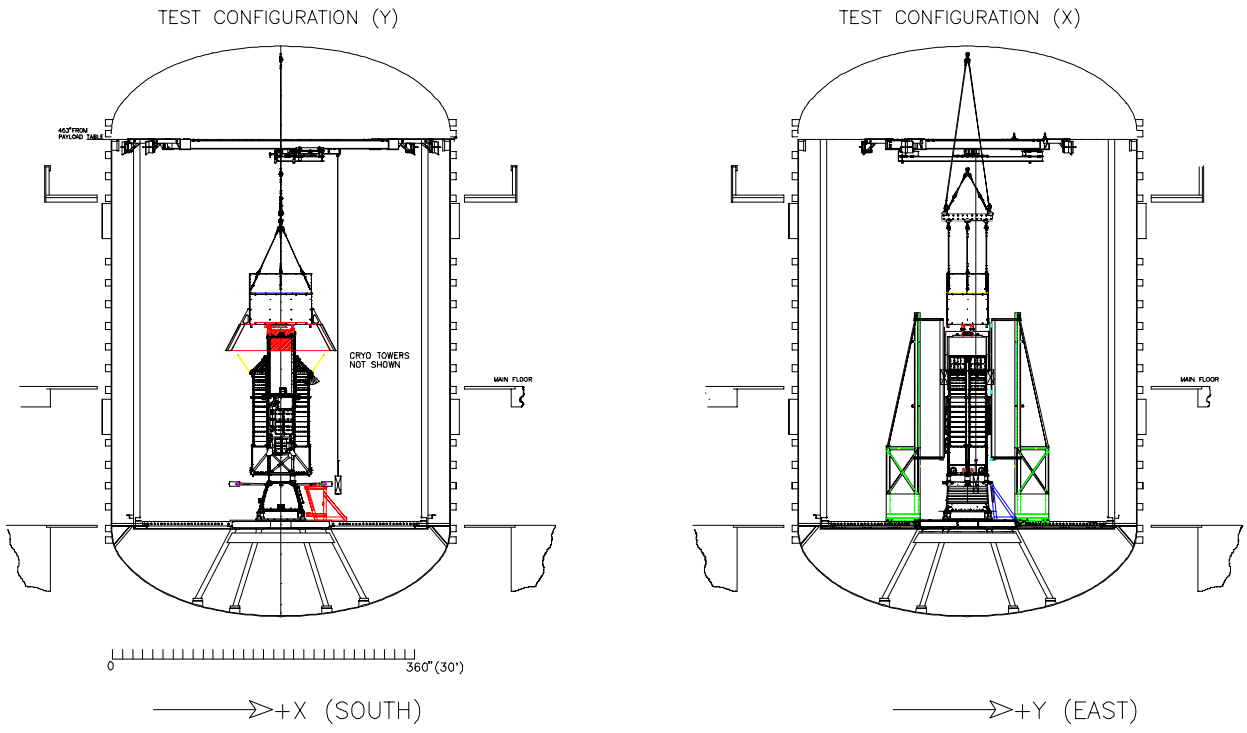

Figure 4. Collimator Assembly in SES

point source imaged back onto the same plane as the source, but center the fiber source on the primary's optical axis. This was accomplished as follows: One person looked through the theodolite while another translated the fiber source until it was centered on the theodolite reticle. The primary mirror adjustment legs were then moved in order to bring the reflected image of the fiber source back on itself. This accomplished the task of placing the primary mirror's optical axis parallel to gravity to approximately 30 arcseconds.

The next and mechanically most difficult step was to install the secondary mirror (Figure 6). This had to be done without disturbing the tube orientation, the lower relay mirror, or the upper relay mirror. Once accomplished, the secondary mirror center could be seen by the theodolite via the upper relay mirror. A small reticle, etched at the center of the secondary mirror, simplified this step. This reticle was a convenient target on which the theodolite operator could sight. The secondary mirror was translated in the two horizontal directions in order to center it on the theodolite crosshairs. The "autocollimation return" from the secondary could then be evaluated. The secondary was adjusted in tip and tilt until this return was centered on the theodolite crosshairs. This process aligned the optical axis of the secondary mirror in decenter, tip, and tilt with that of the primary mirror.

The last step in individual collimator alignment was setting the focus by translating the secondary mirror in piston. The upper relay mirror was removed and the fiber source mentioned previously was moved to the primary mirror cell. It was mounted above the cell on a three-axis translator, placed at the nominal telescope focus position, and configured to illuminate the secondary mirror. The resulting beam from the collimator was reflected via the lower fold mirror to an off-axis parabola (OAP) which was similar to the FUSE primary mirrors in focal length and aperture size (Figure 7). A double pass system was not employed due to difficulty in observing the return image. The OAP imaged this nearly collimated beam onto a surface located near the OAP's focal point. A video microscope was used to view this image and project it on a monitor. The microscope and surface were translated together to produce the smallest possible image. The secondary mirror was then translated in piston in order to bring the image into focus. The microscope and image location and OAP alignment were adjusted iteratively to remove any coma produced by OAP tip/tilt with respect to the incoming beam. The

fiber optic source location and secondary mirror focus were then adjusted in small increments in order to determine the best focus for the collimator. All images were saved using a video capture card linked to the video microscope and a computer.

4.2. Collimator co-alignment

Co-aligning the four collimators was accomplished in two steps (Figure 8). First the four telescopes were mechanically aligned with respect to each other, and second, each source's pinhole was positioned such that it was on the optical axis. The first step was accomplished using standard theodolite metrology methods and the optical cubes on the primary mirror cells.

The optical bench framework was placed on four adjustment jacks. A tilting level was then used to measure the relative heights of the twelve collimator mounting points, and a best fit plane was calculated. The jacks were then adjusted to bring this plane perpendicular to gravity reference. This provided a leveled optical bench from which to start the telescope integration. At this point, an additional optical cube was bonded onto the optical bench and elevation readings of two adjacent faces measured.

After all four telescopes were integrated into the bench, theodolites were placed to autocollimate on the cube faces on each collimator previously measured during the individual alignment. The collimator co-alignment jacks were adjusted to bring the elevation readings of these cube faces to their previous values, thus leveling each collimator optical axis to gravity reference. Each collimator was adjusted in turn until all of the optical axes were parallel to the gravity vector and on a leveled bench. All five optical cubes were then measured with respect to each other in azimuth and elevation to provide a baseline for future stability measurements of the system. This process accomplished the first step of co-aligning the four telescopes.

In order to align the pinhole sources for each collimator, the assembly was lifted, placed on a rotary table, and again leveled to gravity reference via the optical bench cube. This was primarily for convenience in that it allowed us to use a stationary theodolite and rotate the various collimators into position to be measured. The lamp, pinhole, and translation stage were attached to the primary mirror cell approximately at the focal plane of the collimator. A calibrated pentaprism was placed under the collimator of interest such that it projected this star horizontally along the system Yaxis. The theodolite was then adjusted to autocollimate on the front face of the pentaprism in azimuth but set at an elevation perpendicular to the gravity reference. Since the telescope optical axis was parallel to the gravity vector, the pentaprism rotated this axis 90° (perpendicular to gravity). The theodolite imaged the source and the translation assembly was used to bring the star image directly on the theodolite crosshairs. This process was repeated for each collimator in turn, with the result of a leveled optical bench, four telescopes with optical axes parallel to the gravity reference, and four sources placed on the individual telescopes' optical axes.

The only other co-alignment adjustment was to find the focus of each collimator. A CCD camera was mounted on a 5 in. diameter Celestron telescope and a known collimation source was used to pre-set the Celestron-CCD system to focus on a source at infinity. A $\lambda/20$ RMS relay mirror was placed under one of the collimators such that the point source star image was projected horizontally into the Celestron aperture. Images of the star source were recorded as a function of collimator focus. The data were later analyzed to determine best focus for the translator assembly for each individual telescope.

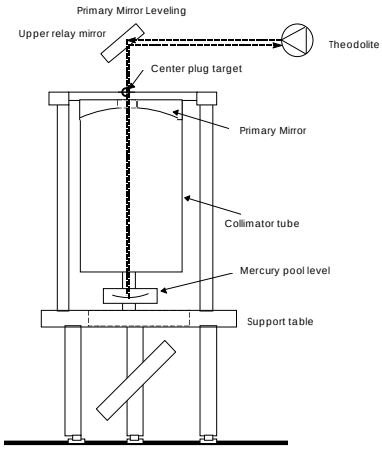

Figure 5 Primary Mirror Leveling

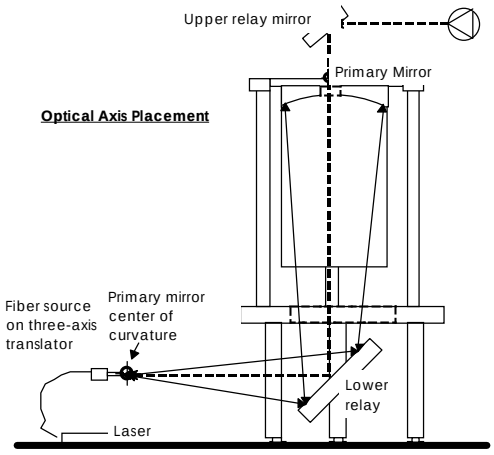

Figure 6 Optical Axis Placement

4.3. Collimator assembly to satellite alignment

The only remaining step was to align the collimator assembly to the FUSE satellite in the vacuum chamber. The close quarters and required work height in the chamber precluded employing standard theodolite metrology, so a simpler method had to be devised to place the collimator optical axis parallel to the FUSE optical axis. Previous metrology of the satellite had leveled the structure such that the instrument optical axis was parallel to gravity reference, but the mounting of the satellite in the SES precluded this method. Two locations parallel to the satellite X- and Y-axes were determined on the spacecraft bus where a precision inclinometer could be placed and an offset from gravity measured. The same inclinometer was then used to measure the offset from gravity of specially fabricated brackets placed on the leveled collimator assembly. In the chamber, the inclinometer was used to measure the same locations on the satellite bus. The orientation of the FUSE optical axis with respect to gravity was calculated from these data, as well as the required offsets of the collimator assembly. The inclinometer was then placed on the collimator assembly brackets and the structure adjusted in tip and tilt until the offset values were obtained.

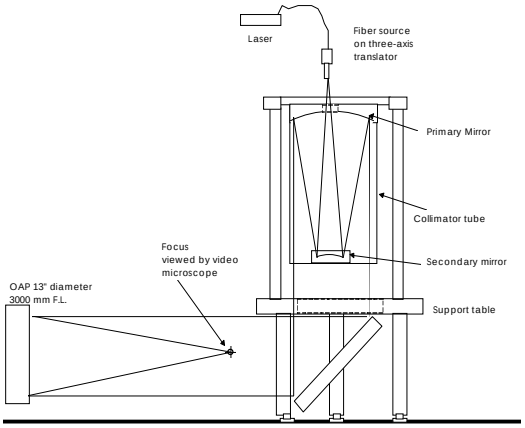

Figure 7 Secondary Mirror Focus and Alignment

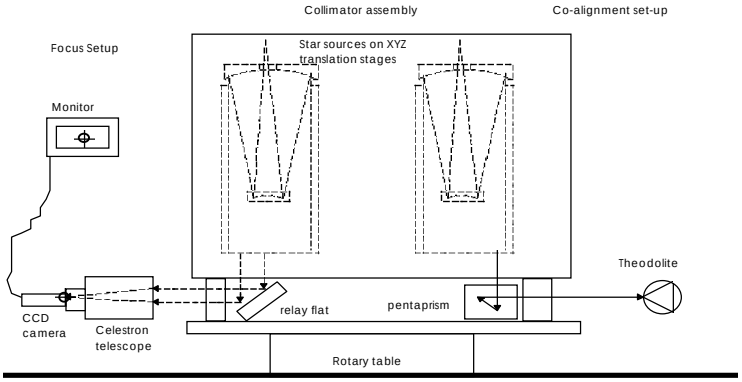

Figure 8 Collimator Coalignment

5. LIGHT SOURCES

Each collimator channel was illuminated by a platinum, hollow-cathode lamp filled with neon gas and sealed with a lithium flouride (LiF) window.* These lamps output visible light as well as a rich spectrum of FUV lines down to the LiF cutoff around 105.0 nm[6], thus providing stimulation for all four UV channels and the visible light fine error sensors (FES). The LiF window cutoff limited the spectral coverage on all instrument channels, but most severely on the two SiC channels where only 20-25% of the channel bandpass was illuminated. However, the coverage was adequate for the purposes of the test, our choices were extremely limited, and this lamp design has a long heritage and well-characterized optical output.[7]

Unfortunately, the geometry of the lamp precludes a low f-number output beam without reimaging optics. The source (hollow cathode) is only 0.10" in diameter and is located 3.2" from the LiF window, resulting in an f/32 beam from a pinhole placed right at the window. The collimators work at f/12. A measurement of the output beam was made at 123.7 nm under N_2 purge, and using the half-power points the angular size of the beam was found to be 1.25°, or about f/23. The faster beam probably results from the lamp discharge being not strictly confined to the hollow cathode diameter.

To increase the speed of the output beam, a customized version of the lamp was designed with a reduced length "neck" (to which the LiF window is bonded), effectively halving the distance from the cathode to the window and, according to our lab test, providing the necessary f/12 output. Unfortunately, difficulties were encountered during manufacture of the custom

* Model NY 10298B, Imaging and Sensing Technology, 300 Westinghouse Circle, Horseheads, NY 14845

lamps due to the proximity of the heat-producing cathode to the sealant at the window bondline. Three custom lamps were delivered in time for the test (one of which was damaged during transport to GSFC for installation -- three more were delivered too late to be tested and installed). We decided to use custom lamps on the two SiC channels and standard lamps on the two LiF channels. To compensate for the significant underfilling of the collimator pupil on the LiF channels, quadruple pinhole apertures were designed and fabricated such that the output beam from each pinhole was directed into a different portion of the pupil. Light from only one pinhole could be directed into the spectrograph slit at any given time; however, by co-adding spectra from all four pinholes, reasonably good coverage of the full aperture was obtained.[8] The multiple pinhole sources could be imaged simultaneously by the visible-light FES cameras, which was beneficial in testing this system.

The output of each lamp was characterized at JHU prior to the test with a system designed to calibrate vacuum-UV light souces. Difficulties with the detector calibration precluded an accurate determination of the spectral output of each lamp, but valuable data were obtained. A 100 μm pinhole was used in front of the lamps; other than this the lamp housing was identical to that used for the OETET. The lamp characterization accomplished several goals:

1. Exercise the lamps under vacuum in actual test configuration.
2. Confirm lamp output down to the LiF window cutoff at 105.0 nm.
3. Provide a rough estimate of expected count rates during OETET.

The count rate estimates matched the observed rates to about 25%. After the test, using this data, a rough instrument efficiency was determined for each channel which matched well with the numbers derived from component-level measurements.[8]

The major problem we encountered with the test hardware was the failure of several lamps. One of the SiC channel lamps (a custom lamp) died after a few hours of runtime during the test. Only an initial collimator focus run had been completed on this channel when the failure occurred, but enough to have seen a spectrum on the detector. The second custom lamp, on the other SiC channel, operated for many hours throughout the first segment of the test, but failed to turn on after backfilling the chamber after the first data run. Our plan was to replace the two failed lamps during the chamber break; however, of the three custom lamps we had in hand, two died during a quick vacuum checkout at JHU and the third failed to turn on at all. This left us no choice but to install two standard lamps which did survive a quick vacuum checkout. Unfortunately, one of these failed to turn on after the second chamber pumpdown; fortunately, it was not on the SiC channel which had suffered the first lamp failure early on.

6. COLLIMATOR PERFORMANCE

The imaging performance of each collimator-flight mirror pairing was measured by producing knife edge distributions (KED) in X and Y by scanning the edge of one of the larger spectrograph slits across the spot. The negative derivative of the KED is the line spread function (LSF), which is a one-dimensional cut through the convolution of the spot with a line source. The LSF in X allows a measurement of slit transmission. The LSFs in X and Y give an indication of spot width and structure. Enslitted energy distributions were also produced by scanning the narrow spectrograph slit across the spot in X.

The observed FUV LSFs for the SiC1 FUSE channel in X and Y are displayed in Figure 9. The estimated flight mirror contribution to each LSF is also shown. The sub-apertured flight mirror's contribution to these LSFs was modeled with the Optical Surface Analysis Code (OSAC),[9] assuming each flight mirror has surface error characteristics similar to the flight spare.[10] We estimated the FWHM of the collimator's contribution to the observed spot by fitting a Gaussian to the OSAC flight mirror contribution and to the LSF data and subtracting in quadrature: $FWHM_{collimator}=\sqrt{(FWHM_{data}^2 - FWHM_{OSAC}^2)}$. This $FWHM_{collimator}$ is listed in Figure 9 and given for each collimator in Table 1.

As is obvious from Figure 9, the spot size is dominated by the FUV collimator PSF, system misalignment and defocus, and/or the finite size of and non-uniform brightness distribution within the slit source at the collimator focus. The uncertainty in focus is approximately +/- 0.5 mm for the f/12 SiC and +/- 2 mm for the f/23 LiF channels. The under-filled entrance pupil, uncertainty in the location of the beam on the flight mirror, and the size of the collimator PSF calls into

question any estimate of system alignment based on spot size. Aperture diffraction is a negligible contribution to spot width, given the FUV wavelengths of interest and the observed spot size.

The LSFs displayed in Figure 9 and the widths given in Table 1 represent lower limits on the width of the collimator PSF in the FUV. The collimators were made to a RMS figure error of 0.035 λ (λ=632.8 nm), but no specification was given for mid-frequency and microroughness errors, which are important to FUV imaging performance.[10] Furthermore, the high f-numbers for the test imply that the effect of figure error on spot size is probably small. The data presented here are limits on the FUV scatter component to the collimator PSF (small-scale surface error is well-sampled even by the tight beam), set by the other potential sources of broadening mentioned above.

A potentially important contribution to the error in these measurements arose from the oscillation of the spot in the focal plane, caused by changing thermal gradients across the aluminum collimator tubes from the thermal control cycling. The oscillation had a ~60 sec. period with an angular amplitude of ~1 arcsecond in X and Y. For a given knife edge or slit position during an imaging test, this caused the signal to vary by as much as a factor of 2 over the course of one period as the spot moved across the occulting edge(s). However, the oscillations were well-sampled for each knife edge/slit dwell position (5--15, 16 sec. integrations). This facilitated the straightforward removal of the oscillation and the calculation of an average signal for each dwell position via a weighted least squares sine fit to the raw data. The error in the estimate of this average signal was of order the error expected from photon statistics for a typical integration.

Imaging data were also obtained later in the OETET (after the custom lamps on the SiC channels were replaced with standard lamps), after an attempt was made to eliminate this oscillation by changing the period of collimator tube heater activation. This lengthened the period of the oscillation considerably, but did not significantly change its amplitude. The oscillations were thus under-sampled and difficult to fit, so these data were not reduced.

Another systematic effect was the frequent "double-binning" of the counts from adjacent 16 sec. integrations, a feature of the OETET electrical ground support equipment . For example, a given set of three integrations might yield 80 counts in 16 sec., then 0, then 160 counts. These sudden changes in the detector signal were numerous, but usually difficult to identify, given the confusion of photon noise and the source oscillation. This effect was generally therefore not removed from the LSF data and contribute significantly to the error bars shown in Figure 9.

Table 1. Collimator FUV Scatter Spot FWHM (Arcseconds)

Channel	SiC1	LiF1	SiC2	LiF2
FWHM X	2.6	2.3	3.1	4.2
FWHM Y	3.4	2.4	3.0	3.8

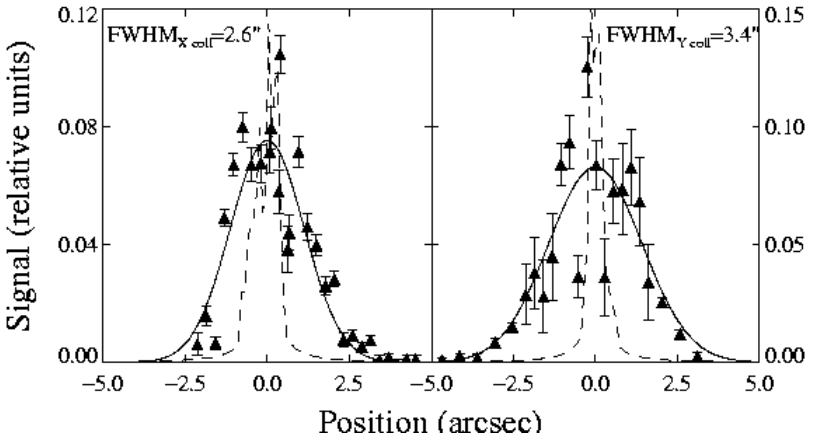

Figure 9. X and Y LSFs associated with the SiC1 FUSE channel (custom lamps) from knife edge data obtained during the OETET (triangles), the OSAC model prediction for the contribution of the flight mirror to the LSF (dashed line), and the estimated (residual) contribution from the SiC1 collimator (solid line). Also listed is the FWHM of the collimator contribution.

7. OETET TEST ACTIVITIES AND FLOW

7.1. Locating the images

The LiF channels of FUSE are each equipped with a FES, which are each equivalent to slit-jaw cameras. Alignment of the image to the slit for these two channels was simply a matter of guiding the image into the known location of the slit in the FES field of view. We employed a spiral search for the SiC channels. This method was much the same as we intend to use in flight, with the exception that the motion of the collimator light source substituted for motion of the satellite. One source was found on the second spiral (~40 arcseconds radially from starting position), and the other on the fifth (~100 arcseconds radially from starting position).

7.2. Focusing the collimators

As we felt we would be unable to decouple the focus of the collimators from that of the flight mirrors, we decided prior to the test to assume that any defocus occurred in the collimators. Focus was determined by scanning the image with a spectrograph slit and recording count rate as a function of slit position, producing KED and LSF data (Section 6). Collimator focus was adjusted, and the scan repeated. As the beam speed was very slow (Section 5), we found the depth of focus to be very large, especially on the channels equipped with the standard lamps. Depth of focus for the standard lamp channels was approximately 2 mm at the collimator, and for the custom lamps about 0.5 mm. The collimators were set to their measured best focus, and left there through the remainder of the vacuum test. After focusing, imaging data were gathered for each channel as described in Section 6.

After the vacuum portion of the OETET, testing of the visible light system revealed a mismatch between the FUV and visible light foci. After significant investigation, it was found that the focus of the collimators varied about 3 mm between vacuum and ambient temperatures. This was of the correct sign and magnitude to explain the apparent mismatch.

7.3. Focusing the spectrograph

Spectrograph focus was determined two ways, both of which are intended to be employed during on-orbit operations. The first method was "slit-less." The spectrograph's 30x30 arcsecond slit was used, as to not obstruct the beam during the focusing. The flight mirror actuators were used to vary the distance between mirrors and gratings until the spectral features were narrowest. This method only worked well on the channel equipped with custom lamps, the result of depth of focus issues.

The second method projected light through the 1.25x20 arcsecond spectrograph slits, and used the flight motions of both the slits and mirrors to adjust mirror to grating distance. For the standard lamp channels, multiple lamp pinhole apertures were used to illuminate different places on the mirrors, and focus adjustments were made until the same spectral features from beams hitting different parts of the FUSE entrance pupil were made to overlap on the detector in the dispersion direction. This method was also found to work well. Both focusing methods are planned for in-flight spectrograph focusing, and are expected to give the same result.

7.4 Other characterization tests

Other UV characterization tests included measurements of spectrograph slit transmission, a rough estimate of system efficiency, and detector thermal stability. Ratios of energy transmitted through each spectrograph slit were used to generate some weak verification of imaging performance (mid-frequency scatter would not be affected by our limited beam speed; Section 6). System efficiency was determined via the calibration of lamp and pinhole FUV output, combined with the measured reflectivity of collimator witness mirrors. While this type of measurement necessarily has very large errors, our goal was to establish that FUSE did not have any problems severe enough to cause a great loss of science return. System thermal stability was tested by varying instrument temperatures while monitoring optical performance. We were not able to conclusively show coalignment stability during temperature change, as collimator-to-FUSE mirror alignment varied with temperature (Section 6).

7.5 Support for flight simulation testing

One of the most important services the optical stimulation system provided was a "star field" of visible and FUV sources for flight simulation testing. These consisted primarily of two types, "orbits" tests and mission simulations. Orbits testing was primarily for the attitude control system of the FUSE satellite. Sources were moved in and out of the spectrograph slits, and around the field of view of the FES in order to simulate acquiring targets in-flight. Mission simulations were intended to exercise the system by fully imitating orbit activities, including use of the mission operations center at The Johns Hopkins University.

7.6 Test flow

Our test flow was broken up over approximately 8 weeks of vacuum operations. While the order of testing very roughly followed the listing above, it was interspersed with other, non-optical testing. Approximately one-third of the total time spent under vacuum was devoted to optical testing, while another third was devoted to flight simulation.

8. CONCLUSION

While the test suffered from severe weaknesses, primarily as a result of using lamps not matched to our system, we generally consider the OETET to be highly successful. As a result of the test, an opto-mechanical problem caused by the instrument secondary mechanical structure's coupling to the optical bench was uncovered. This coupling significantly defocused the spectrograph, and translated the spectra in the cross-dispersion direction. The mechanical engineering team implemented a fix during a break in vacuum testing, and additional vacuum FUV testing verified its success. This problem would have severely compromised the science return of the FUSE mission if left undetected. This result alone was worth the investment put into the OETET.

Additionally, we successfully showed:

- FUSE system efficiency was approximately what we expected from component level testing.
- Spectral resolution was consistent with that measured during spectrograph optical testing at the University of Colorado.[11]
- Our methods for on-orbit focusing and aligning the instrument are effective.
- The FUV detectors operate in the system under flight-like conditions.

We were unable to measure system imaging performance. We will rely on a combination of component level measurements and analysis to verify this performance requirement. Other weak points were the verification of the ability of FUSE to focus to a source at infinity using the flight actuators and demonstration of maintaining coalignment during temperature change.

Some lessons learned are described below.

8.1. Schedule

As is usual during thermal vacuum testing, operations were conducted 24 hours a day, 7 days a week. The optical portion of the pre-test schedule was about 14 days of the 40 days scheduled under vacuum. As run, optical testing was approximately 20 days of the total 56 days under vacuum.

8.2 Cost

The cost of developing the required hardware for this activity was significantly higher than originally budgeted --- very approximately double. This was caused by continual increase in the complexity of the collimator system, brought on by problems encountered during the design and fabrication process. During the cost estimation process, we severely oversimplified the system.

8.3 Procedure

A very detailed procedure was developed in advance of the OETET.[12] Producing this procedure was critical to communicating the methods to be employed to the wide variety of personnel supporting the test. During the test itself, record keeping was generally done using laboratory notebooks. This was more appropriate than using the procedure, as the methods were continually refined, and certain steps repeated multiple times.

8.4 Errors Made

A number of errors were made on our part which were, in general traceable to early oversimplifications and assumptions. The three most glaring errors were not matching the lamps to our optical system, not making enough effort to focus the collimators in advance of the test, and not designing the test adequately to monitor coalignment motions of the instrument during simulated orbital thermal changes. The first two errors, while discovered prior to the actual test, were not corrected primarily for perceived schedule limitation reasons. In hindsight, the actual test occurred later in time than expected, and this could have allowed time to correct both of these problems.

Our learning curve during this activity was very steep, caused by both running tests that could not be simulated in advance, and lack of experience with all aspects of the satellite operations. This was the first opportunity to operate the satellite in a "flight like" manner.

ACKNOWLEDGEMENTS

FUSE is supported through the Explorers Program office at Goddard Space Flight Center, and managed within the Center for Astrophysical Sciences at The Johns Hopkins University. The authors would like to thank Jordan Evans, Tim Horner, Joe Orndorff, Tom Reeves, Vicki Roberts, Louis Worrel, Judy Yienger, and the FUSE electrical test team for their support of this work. We also gratefully acknowledge Dr. Timo Saha of NASA/Goddard Space Flight Center for the OSAC modeling presented in Section 6. This work was supported by NASA contract NAS5-32985.

REFERENCES

[1] J. Green, E. Wilkinson, and S. Friedman, "The design of the Far Ultraviolet Spectroscopic Explorer spectrograph," SPIE, vol. **2283**, pages 12-19, 1994.

[2] E. Wilkinson, J. Green, S. Osterman, K. Brownsberger, and D. Sahnow, "Integration, Alignment, and Initial Performance Results of the *Far Ultraviolet Spectroscopic Explorer* (FUSE) Spectrograph," SPIE, vol. **3356**, pages 18-29, 1998.

[3] S. Conard, K. Redman, R. Barkhouser, and J. Johnson, "Optical alignment of the Far-Ultraviolet Spectroscopic Explorer (FUSE)," SPIE, vol. **3765**, 1999 (this volume).

[4] National Aeronautics and Space Administration, *Engineering Services Division Facilities & Capabilities*, Goddard Space Flight Center internal publication, pages 142-145 (1995).

[5] M. Ruda, *Introduction to Optical Alignment Techniques*, class notes from College of Engineering, University of Wisconsin-Madison.

[6] J.F. Osantowski, R.A.M. Keski-Kuha, H. Herzig, A.R. Toft, J.S. Gum, and C.M. Fleetwood, "Optical coating technology for the EUV," Adv. Space Res. **11**, 185--201 (1991).

[7] J. Z. Klose, G. F. Hartig, and W. J. Rosenberg, "Characterization of a Pt-Ne hollow cathode spectral line source", *Appl. Opt.* **29**, pp. 2951-2959, 1990.

[8] S. Friedman, S. Conard, R. Barkhouser, A. Cha, A. Fullerton, J. Kruk, E. Murphy, R. Ohl, D. Sahnow, H. Weaver, K. Brownsberger, "Pre-launch optical tests and performance estimates of the far-ultraviolet spectroscopic explorer satellite," SPIE, vol. **3765**, 1999 (this volume).

[9] R. Noll, P. Glenn, J. Osantowski, "Optical surface analysis code (OSAC)," SPIE **62**, pp. 78-82, 1983.

[10] R. Ohl, S. Friedman, T. Saha, R. Barkhouser, H.W. Moos, "Optical testing of the far-ultraviolet spectroscopic explorer (FUSE) primary mirrors and predicted on-orbit performance," SPIE, vol. **3765**, 1999 (this volume).

[11] A. Cha, D. Sahnow, H.W. Moos, "Processing and interpretation of pre-flight FUSE spectra," SPIE, vol. **3765**, 1999 (this volume).

[12] S. Conard "FUSE Satellite Optical End-to-End Test," FUSE-TAP-1020, Rev A, FUSE internal document.